Optimized tubular radiator with annular fins on a nonisothermal base

S. Sunil Kumar* and S. P. Venkateshan
Indian Institute of Technology, Madras, India

In this paper, a large-scale computational analysis has been undertaken of tubular radiators with fin arrays in which the temperature of the fluid varies along the radiator length. The presence of an optimum fin outer diameter for a given pipe diameter, which is independent of other thermophysical parameters, has been brought out. A set of useful correlations, which will enable the designer to quickly evaluate the performance of the system, is developed for different fin profiles. A design methodology assuming an infinite fluid side heat transfer coefficient has been presented. Comparisons have been made for validating the present calculations.

Keywords: incidence equations; heat loss ratio; fin profiles; fin volume; optimum fin radius

Introduction

The use of extended surfaces for augmenting heat transfer in space applications is well known. In the absence of convection, radiation coupled with conduction is the only mode of heat transfer. At present, the design trend in such systems is to arrive at a weight-optimized design on a viable fin geometry. Sparrow et al. (1961) and Karlekar and Chao (1963) considered mutual irradiation between the fins but neglected base interaction for a radiator with longitudinal fins on a cylindrical base. Sparrow et al. (1962) analytically studied the heat transfer characteristics of an annular fin and tube radiator. They fully accounted for the complex interaction problem resulting from the mutual irradiation between neighboring fins and between fins and tube surfaces by applying the then newly devised contour integral method (Sparrow 1962) for deriving the radiant interchange factors. The results definitely indicate that the use of fins lead to a significant increase in heat transfer compared with the unfinned tubular radiator. Schnurr (1976) devised an optimization technique for radiating fin arrays with respect to weight. Here, a nonlinear optimization approach is used to determine the minimum weight configuration for the radiating fin arrays used in space applications. Straight and circular fins of rectangular and triangular profiles were considered. Except for the optimization technique, the analysis of the problem resembles the earlier work of Sparrow et al. (1962).

Keller and Holdredge (1970) obtained a one-dimensional (1-D) numerical solution for the steady-state thermal behavior of annular fins of trapezoidal profile that transfers heat by conduction and radiation. Schnurr and Cothran (1974) developed a numerical method to calculate the temperature distribution and radiant heat transfer for an annular fin tube radiator with fins of trapezoidal profile. All surfaces were assumed to be gray and to emit and reflect diffusely. Radiative interactions between adjacent fins and between fins and tube were included. Results of a parametric study for the special case of circular fins of triangular profile, with constant thermal conductivity were presented and were used to optimize the fin array with respect to weight.

Sunil Kumar et al. (1992, 1993) have considered rectangular and trapezoidal profiled fins standing on a surface that forms the side of a duct through which hot fluid is flowing. The analysis was made for a radiator with varying base temperature, thus accounting for the variation of temperature of the coolant flowing in the duct. An optimization technique was devised to find the maximum heat loss for a given volume addition, along with a method to find out the minimum weight required for a given heat loss. A parametric study was carried out, and correlations were evolved to find the optimum fin number and maximum heat loss ratio.

The present analysis is directed towards an annular finned radiator where the working fluid inside the tube changes its temperature as it flows inside the tube, losing heat into space due to radiation from the tube surface (and from the annular fins, if they are present). This geometry and assumption represent a true radiator and are a departure from all the above-mentioned references, which have assumed a constant fin base temperature. The geometry involves the interaction of radiation between a nonisothermal fin with neighboring nonisothermal fins, nonisothermal base, and a constant temperature environment. Since the problem is highly nonlinear and conjugate in nature, the computer time needed for the solution is very large. Consequently, the parametric study is restricted to four parameters only, namely the $\dot{m}Cp$ product, inlet temperature, added fin volume, and the pipe diameter. This restriction is accomplished by keeping the emissivity of all radiating surfaces constant at 0.98 (for lacquer paints) and by keeping the root thickness of the fin constant at 0.15 cm, which is assumed to be sufficient to withstand forces during take off and maneuvering of the spacecraft of which the radiator is a part. The whole fin system and the tube are made of aluminum with a thermal conductivity of 207 W/mK.

In the following analysis, a term called the heat-loss ratio, defined as the ratio of heat loss from the finned radiator to that from an unfinned radiator (Sunil Kumar et al. 1992, 1993) is evaluated, and its dependence on the other thermophysical parameters is brought out. The existence of an optimum outer

* Presently with Tata Energy Research Institute, New Delhi, India. Address reprint requests to Professor Venkateshan, Indian Institute of Technology, Dept. of Mechanical Engineering, Madras 600 036, India.

Received 7 June 1993; accepted 18 April 1994

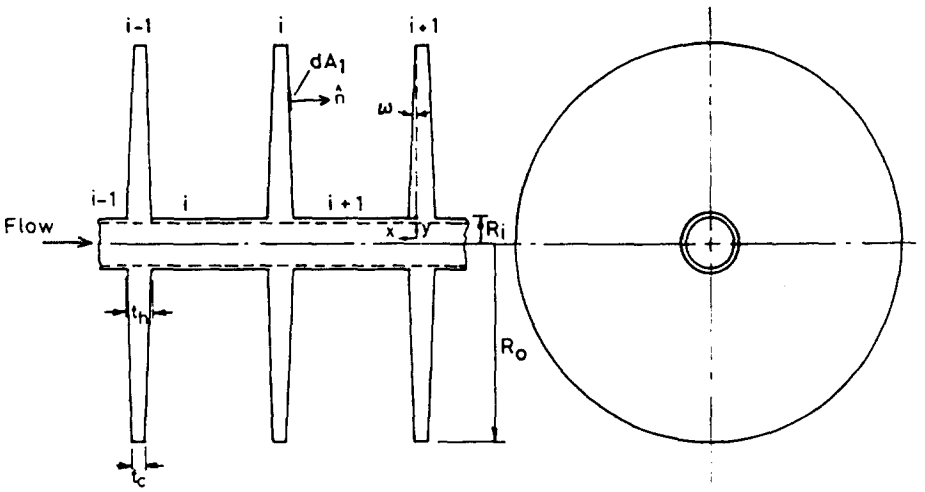

Figure 1 Nomenclature for a tubular radiator with annular fins of trapezoidal profile

diameter of the fin irrespective of the other thermophysical parameters such as ε, T_{in}, and mCp for a given pipe diameter is brought out from a detailed analysis. Finally, correlations are arrived at for three fin geometries (triangular, trapezoidal, and rectangular) for a quick evaluation of the performance of the radiator. A straightforward optimization technique within the range of parameters discussed earlier is also presented.

Statement of the problem

The radiator under consideration is a tube carrying a hot fluid, with annular fins of trapezoidal profile around it, as shown in Figure 1 (extreme cases are triangular and rectangular profiles), and losing heat to outer space by radiation alone. The base lengths to the left of the first fin and to the right of the last fin are selected such that they are equal to half the spacing between any two intermediate fins. All surfaces are diffuse and have a uniform emissivity of ε. The basic difference between a condenser/evaporator and a radiator is that while the temperature of the coolant stays constant in the case of the former, it varies in the case of the latter. Consequently, the assumption of identical temperature profiles for all the fins cannot be made, as in the earlier works. Analysis of each fin has to be done separately. Each fin will have one energy equation and two incidence equations, one for the right side and the other for the left side of the fin surface. The energy equation on the fluid side is also to be incorporated in the analysis. All this will result in a set of nonlinear integro-differential equations.

Notation

Cp	Specific heat of the fluid, J/kg.K
dF	Diffuse view factor
g	Irradiation, W/m^2
k	Thermal conductivity of the fin material, W/m.K
l_1	Length term as defined by Figure 3a
L	Length of the radiator, m
m	Mass flow of fluid, kg/s
n	Number of fins
N_{CC}	Convection conduction interaction parameter, nondimensional = (m.Cp)/k.L
N_g	Geometrical factor = $1 + (t_i/(2.R_i.\tan\omega))$
N_i	Radiation conduction interaction parameter for fin $i = (\varepsilon.\sigma.T_{bi}^3.R_i/k)$
N_{RC}	Black-body fin radiation conduction interaction parameter, nondimensional = $(\sigma.T_{in}^3.R_i)/k$
N_{RF}	Radiation convection interaction parameter, nondimensional, $(\varepsilon.\sigma.T_{in}^3.2.\pi.R_i)/(m\text{Cp})$
P	Nondimensional fin radius = R_i/R_o
q	Heat loss from the unfinned radiator, W
R_i, R_o	Fin inner and outer radius, m
r_{OPT}	Scaled optimum fin number parameter, nondimensional, $(1 + n.(R_0 - R_i)/L)$
r_1	Radius of the element on the fin, m
S	Fin spacing, m
t_h, t_c	Base and tip fin thickness, m
T	Fin temperature, K
T_b	Base temperature, K
T_{in}	Fluid temperature at inlet, K
V	Volume of fin added, m^3
x	Coordinate variable along the base, m
y	Coordinate variable along the fin, m

Greek symbols

β	Nondimensional heat loss from the unfinned radiator, $q/(2.\pi.R_i.\varepsilon.\sigma.T_{in}^4.L)$
ε	Emissivity of all exposed radiating surfaces
ψ, ρ	Angle terms as defined in Figures 2 and 3b
σ	Stefan–Boltzmann constant, 5.67×10^{-8}W/m^2.K^4
θ	Nondimensional temperature, T/T_{bi}
ρ	Nondimensional coordinate along the radius of the fin = r_1/R_i
φ	Heat-loss ratio, nondimensional
ω	Angle defined as in Figure 1

Subscripts

b	Base
e	Opening to the space
i	Fin number
j	Base between $(i-1)$th fin and ith fin
L	Left surface of the fin
R	Right surface of the fin
∞	Environmental condition
1, 2	Neighboring fins 1 and 2

Formulation

Although the formulation of the problem here shares a few common features with that of the one in Sunil Kumar et al. (1993), the geometry of the problem makes the analysis more tedious. The crossed-string method could be used for the evaluation of view factors in the previous analysis of the two-dimensional (2-D) duct type geometry. However, due to the finiteness of the elements involved, the irregular shapes, and the shading effect of the tube on the fin surfaces, in the present geometry all relevant shape factors are to be evaluated numerically by the contour integral method.

Basic assumptions

Heat loss from the surface is strictly by radiation alone. Formulation of the problem is carried out at steady state with an outer space temperature of 0 K and material surfaces having an emissivity of ε. The local temperatures of the fins are assumed to be constant across the thickness. Hence the fin heat transfer is treated as 1-D, and the temperature variation is only in the radial direction. At the tip, the heat conducted is equated to the heat loss by radiation. Resistance of the walls and the film on the liquid side of the heat exchanger are negligible, since the normally used fluids like the liquid metals have high heat transfer coefficients. Fluid flow is fully developed, and local fluid bulk temperature is assumed to be equal to the local base temperature.

Energy balance

For the present analysis, a volume element $r_1 d\psi . dr_1 . t$ bounded by a surface area dA_1 is selected, which when rotated generates a ring element, as shown in Figure 2. The differential equation resulting from an energy balance for such an element in the ith radiating conducting fin, in the nondimensional form, is given by

$$\frac{d^2\theta_i}{d\rho^2} + \left[\frac{2\rho - N_g}{\rho^2 - N_g.\rho}\right]\frac{d\theta_i}{d\rho} + \frac{N_i}{(\rho - N_g)2.\tan\omega} \times \left\{2\theta_i^4 - \left[\frac{q_{i,R} + q_{i,L}}{\sigma T_{bi}^4}\right]\right\} = 0 \quad (1)$$

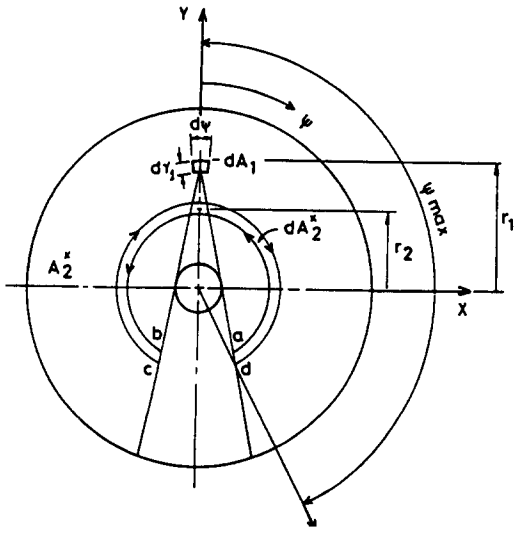

Figure 2 Geometry for radiant interchange between area elements on two adjacent fins in the tubular radiator

with boundary conditions

$$\rho = 1,\ \theta_i = 1, \text{ and} \quad (2)$$

$$\rho = R_0/R_i,\ d_\theta/d\rho = -N_i.\theta_i^4$$

In order to determine the temperature along the base, the above equations are combined with the energy balance on the fluid side, viz.,

$$m\mathrm{Cp}(T_{in} - T_{bi}) = q_r \quad (3)$$

where q_r is taken as the heat lost up to the ith fin along with the heat lost by the left surface of the fin. Before going into the two incidence equations, one for the right and the other for the left side of the fin, it is necessary to carry out a shape factor analysis for the different elements involved in exchange of radiation.

Consider an elemental area dA_1 on the fin (shown in Figure 2) that exchanges radiation with the left and right fins, with space, and with the base. Because of the shielding action of the tube surface, radiant energy from only a portion of the opposite (left or right) fin is able to strike the element dA_1. This area can be found by drawing tangents from dA_1 to the tube surface (shown in Figure 2). Since the temperature along the radius of this area is varying, we divide this into small isothermal elemental areas of truncated rings dA_2^*, as shown in Figure 2.

The second surface that exchanges radiation with dA_1 is the tube surface. The portion of the tube surface that is in radiant interaction is again found by drawing tangents from dA_1 to the tube surface, as shown in Figure 3a. The participating base surface area is denoted by A_b^*. This area is also divided into a number of isothermal elements of area dA_b^* for shape factor calculation.

Angle factor evaluation

The method uses a contour integration representation of shape factor wherein the area integrals are converted into line integrals. The evaluation can first be made for the shape factor from the area element dA_1 to the truncated ring element dA_2^* on the adjacent fin. The origin of the coordinates is fixed at the point shown in Figure 2. The location x_1, y_1, z_1 represents the position of dA_1, and x_2, y_2, z_2 represents a point on the contour of the ring element dA_2^*.

From Sparrow (1962), the expression for the shape factor from dA_1 to dA_2^* is given by $dF_{dA_1 - dA_2^*} = l.C_l + m.C_m + n.C_n$, where the C's represents the contour integrals over dA_2^*. Directional cosines l, m, n, in this case are $l = 0$, $m = \cos(90 - \omega)$, $n = \cos(180 - \omega)$. Therefore,

$$2.n.dF_{dA_1 - dA_2^*} = m.\oint \frac{(x_2 - x_1).dz_2 - (z_2 - z_1).dx_2}{r^2} + n.\oint \frac{(y_2 - y_1).dx_2 - (x_2 - x_1).dy_2}{r^2} \quad (4)$$

The contour is subdivided into segments ab, bc, cd, and da for convenience of integration. Since the integrands over the segment $a - d$ and $c - b$ are infinitesimally small compared to the other two, it is enough to integrate over the circular arcs $d - c$ and $b - a$ alone. Now, for the area dA_1,

$$x_1 = 0,\ y_1 = r_1,\ z_1 = s + (r_1 - R_i).\tan\omega + (R_o - R_i).\tan\omega$$

Similarly, for the contour $b - a$,

$$x_2 = r_2.\sin\varphi,\ y_2 = r_2.\cos\varphi,\ z_2 = (r_2 - R_i).\tan\omega$$

where φ varies from $-\varphi_{max}$ to $+\varphi_{max}$.

Also, $dx_2 = r_2.\cos\varphi.d\varphi$, $dy_2 = -r_2.\sin\varphi.d\varphi$, $dz_2 = 0$. For the curve $b - a$, noting the symmetry of the curve, the integral

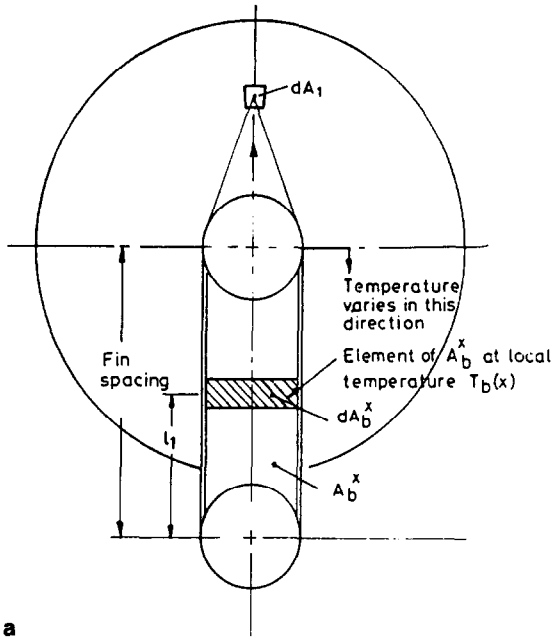

Figure 3a Geometry for radiant interchange between a fin element and a base area

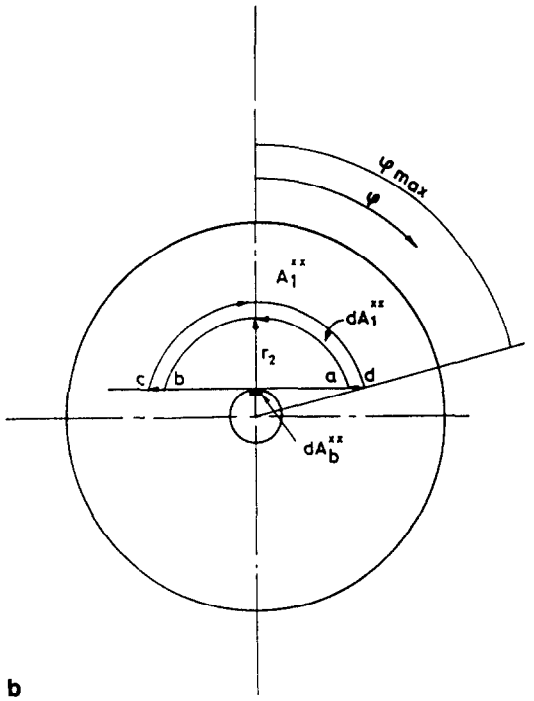

Figure 3b Geometry for interchange of radiant energy between an element on the base tube and an element on the fin

over $b - a$ can be written as

$$I = 2m.[s + (r_1 - r_2 - R_i + R_0).\tan\omega].\int_0^{\varphi_{max}} \frac{r_2.\cos\varphi.d\varphi}{r^2} + 2n.\int_0^{\varphi_{max}} \frac{(r_2^2 - r_1 r_2\cos\varphi).d\varphi}{r^2} \quad (5)$$

where

$$r^2 = r_2^2 + r_1^2 - 2r_1 r_2.\cos\varphi + [s + (r_1 - r_2 - R_i + R_0).\tan\omega]^2$$

and

$$\varphi_{max} = \cos^{-1}(R_i/r_1) + \cos^{-1}(R_i/r_2)$$

This integral can be evaluated numerically. It can be seen that the desired elemental view factor is obtained by differentiating the above expression with respect to ρ_2. Hence,

$$dF_{dA_1 - dA_2^*} = -(1/2\pi).(\partial I/\partial\rho_2).d\rho_2 \quad (6)$$

which also can be evaluated numerically.

The angle factor $dF_{dA_1 - dA_b^*}$, representing the fraction of energy emitted by dA_1 that strikes on the convex surface dA_b^* shown in Figure 3a, can be found using the expression given by Sparrow et al. (1962), which is for the entire length of the base (that is, between two adjacent fins). Here the surfaces involved in the radiant interchange are at right angles to each other. To get the desired results for the present geometry, the expression given therein must be multiplied by $\cos\omega$. Elemental view factor $dF_{dA_1 - dA_b^*}$ may be obtained by shape factor algebra coupled with the expression given by Sparrow et al.

The third view factor that has to be evaluated is the one from the circular ring element on the base to the fin. This can be carried out by discretizing the circular base element into a number of infinitesimal areas dA_b^{**}, as shown in Figure 3b. It is clear from Figure 3b that this area will see A_1^{**} on an adjacent fin. This area can be divided into a number of truncated circular rings of area dA_1^{**}. Now the view factor calculations are done for the element dA_b^{**} to dA_1^{**}. Let x_1, y_1, z_1 represent the location of dA_b^{**} and x_2, y_2, z_2 represent a point on the contour of the truncated ring dA_1^{**}. With the coordinate axes, as shown, we have

$$x_1 = 0,\ y_1 = 0,\ z_1 = l_1$$

and

$$x_2 = r_1.\cos\psi,\ y_2 = r_1.\cos\psi,\ z_2 = s + (r_1 - 2R_i + R_0).\tan\omega$$

Here $l = n = 0$, $m = \cos(0) = 1$, and the ψ value varies from zero to $\psi_{max} = \cos^{-1}(R_i/r_1)$, taking into account the symmetry of the ring. The final expression for the view factor is

$$2.n.dF_{dA_b^{**} - dA_1^{**}} = m.\oint \frac{(x_2 - x_1).dz_2 - (z_2 - z_1).dx_2}{r^2} \quad (7)$$

where $r^2 = r_1^2 + [s + (r_1 - 2R_i + R_0).\tan\omega - l_1$.

For the contour $a - b$, the integrand becomes

$$I = 2.[l_1 - (s - 2R_i + R_0).\tan\omega].\int_0^{\psi_{max}} \frac{r_1.\cos\psi.d\psi}{r^2} \quad (8)$$

Therefore, following the previous argument used to find out the value of $dF_{dA_1 - dA_2^*}$, we have

$$dF_{dA_b^{**} - dA_1^{**}} = (-1/2\pi).(\delta I/\delta\rho_1).d\rho_1 \quad (9)$$

which again is to be calculated numerically.

The remaining view factors can be calculated as follows. The view factor from dA_1 to the opening, A_e is

$$F_{dA_1 - A_e} = 1 - (F_{dA_1 - A_b^*} + F_{dA_1 - A_2^*}) \quad (10)$$

Similarly, the view factor from dA_b^* to the opening, A_e, is

$$F_{dA_b^* - A_e} = 1 - (F_{dA_b^* - A_1} + F_{dA_b^* - A_2}) \quad (11)$$

The value of $F_{dA_b^{**} - A_e}$ can similarly be determined.

Incidence equations

The two incidence equations, one for the right and the other for the left side of the ith radiating conducting fin, can be

written as follows. The incidence equation for the right side of the fin is given by

$$g_{i,R} = \alpha.T_\infty^4.dA_1.F_{dA_1-A_e} + \left[\varepsilon.\sigma.\int_0^S T_{b_{i+1}}(x)^4 + (1-\varepsilon).\sigma. \times \int_0^S T_\infty^4.dA_b^*.F_{dA_b^*-A_e}\right].dA_1.dF_{dA_1-dA_b^*}$$

$$+ 2\pi.\left[\varepsilon.(1-\varepsilon).\sigma.\int_{R_i}^{R_0}\int_0^S T_i(r_1)^4 + T_{i+1}(r_1)^4) + (1-\varepsilon)^2.\int_{R_i}^{R_0}\int_0^S g_{i,R}(r_1) + g_{i+1,L}(r_1)\right]$$

$$\times -dA_b^{**}.dF_{dA_b^{**}-dA_1^{**}}.dA_1.dF_{dA_1-dA_b^*}$$

$$+\left[\varepsilon.\sigma.\int^{R_0} T_{i+1}(r_1)^4 + (1-\varepsilon). \times \int_{R_i}^{R_0} g_{i+1,L}(r_1)\right].dA_1.dF_{dA_1-dA_2^*} \quad (12)$$

For the left surface of the fin,

$$g_{i,L} = \sigma.T_\infty^4.dA_1.F_{dA_1-A_e} + \left[\varepsilon.\sigma.\int_0^S T_{b_i}(x)^4 + (1-\varepsilon).\sigma. \times \int_0^S T_\infty^4.dA_b^*.F_{dA_b^*-A_e}\right].dA_1.dF_{dA_1-dA_b^*}$$

$$+ 2\pi.\left[\varepsilon.(1-\varepsilon).\sigma.\int_{R_i}^{R_0}\int_0^S (T_i(r_1)^4 + T_{i-1}(r_1)^4) + (1-\varepsilon)^2.\int_{R_i}^{R_0}\int_0^S g_{i,L}(r_1) + g_{i-1,R}(r_1)\right]$$

$$.dA_b^{**}.dF_{dA_b^{**}-dA_1^{**}}.dA_1.dF_{dA_1-dA_b^*}$$

$$+\left[\varepsilon.\sigma.\int_{R_i}^{R_0} T_{i-1}(r_1)^4 + (1-\varepsilon). \int_{R_i}^{R_0} g_{i-1,R}(r_1)\right].dA_1.dF_{dA_1-dA_2^*}$$

These two equations are derived using the incident energy equation on a circular elemental ring on the tube, i.e., irradiation on the base, viz.,

$$g_{b,i}(x) = \sigma.T_{4\infty}.dA_b^{**}.F_{dA_b-A_e} + \varepsilon.\sigma.2\pi.\left[\int_{R_i}^{R_0}\{T_{i-1}(r_1)^4 + T_i(r_1)\}\right].dA_b^{**}.dF_{dA_b^{**}-dA_1^{**}}$$

$$+ (1-\varepsilon).2\pi.\left[\int_{R_i}^{R_0}\{g_{i-1,R} + g_{i,L}\}\right].dA_b^{**}.dF_{dA_b^{**}-dA_1^{**}} \quad (14)$$

Method of solution

The numerical solution procedure used here is similar to the one used by Sunil Kumar et al. (1993) for the flat-duct-type radiator with fins. For the sake of completeness, a brief summary of the method is given here. Assuming uniform base temperature, initial solution for the fin equations are found by setting the irradiation values to zero. Using the fin temperature profiles thus obtained and the previous values of base temperatures, new irradiation values are found. Base temperatures are updated, using these irradiation values and the energy equation on the fluid side. With these newly calculated base temperatures and the previously computed irradiation values, new fin temperature profiles are determined by solving the fin equation. This procedure is continued until a desired convergence is achieved for the outlet temperature. Equations 1 and 2 are solved by the second-order Runge–Kutta method. A convergence criterion of 0.0001 on the nondimensional temperatures is selected. All the integrals are evaluated using Simpson's rule. For the overall iteration for the radiator, the outlet temperature is required to converge with a maximum absolute error of 0.001.

Results and discussions

Calculations were initially made to check the accuracy of the present numerical solution procedure and the present formulation of the problem. It was found that the calculations carried out for a constant tube surface temperature radiator agreed with the calculation of Sparrow et al. (1962). Also, in the nonisothermal base case, as the value of mCp is increased, the base temperature tends to progressively attain a uniform value. This can be appreciated from Figure 4, where the heat loss from the system is plotted against inlet temperature. It can be seen that as the mCp value is increased, the system performance approaches that of a condenser, as studied by Sparrow et al. (1962).

Since the number of parameters in such a system is large and the computer time required per set is enormous, calculations have been restricted to a single value of emissivity of 0.98 (lacquer paints). The system is assumed to be fabricated from aluminum, and hence the thermal conductivity is held fixed at 207 W/mK in all the calculations. The length of the radiator is varied from 0.5 m to 1 m. Inlet temperature is varied from 350 K to 550 K in suitable steps. This range covers the values encountered in satellite applications. The mCp value is varied from 2 W/K to 15 W/K. The fin root thickness was restricted to 0.0015 m with three different fin profiles, *viz.*, 1) triangular ($t_c/t_h = 0$), 2) trapezoidal ($t_c/t_h = 0.5$), and 3) rectangular ($t_c/t_h = 1$).

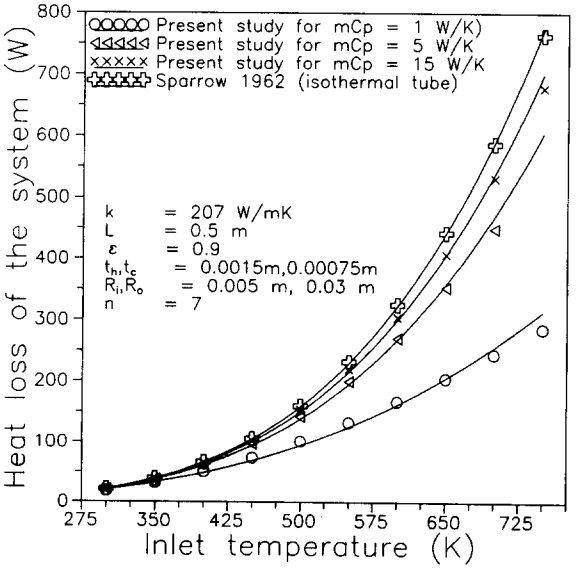

Figure 4 Variation of system heat loss with fluid inlet temperature for various mCp values

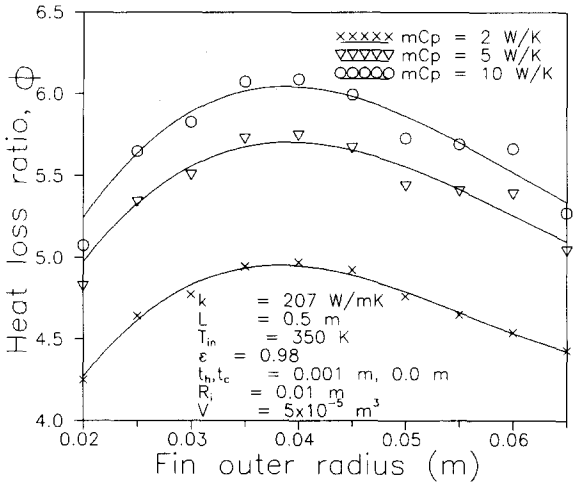

Figure 5 Plot of heat loss ratio vs. fin outer radius with *m*Cp as a parameter. Optimum fin outer radius is independent of *m*Cp

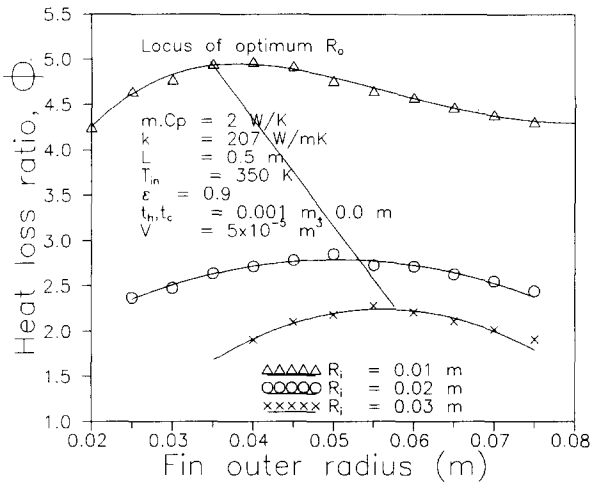

Figure 6 Existence of an optimum fin outer radius for base tubes of different radii. The locus of the maxima lie on a straight line

Before launching on a detailed numerical study, a few calculations were made to elucidate the effect of the fin outer diameter on the heat-loss ratio for the case of triangular profiled fins. It was immediately found that there is invariably a maximum heat-loss ratio for an optimum fin-tip diameter for a given tube diameter, which is independent of the emissivity of the surface, *m*Cp value, and the inlet temperature. The typical heat loss ratio variation is as shown in Figure 5, where the optimum heat loss takes place for a fin outer radius of 0.04 m, independent of the *m*Cp value. Further it was found that this optimum is not influenced by the added volume due to fins. This result indicates that the optimum is influenced strongly by the geometric factors and to a smaller extent by the thermophysical parameters. The only parameter that decides the outer diameter is the tube radius. Calculations performed for a different tube radii showed that the optimum outer radius tends to increase with tube radius, as shown in Figure 6. Curiously, in all these cases it was found that the optimum heat loss occurs when the fin height is around 0.025 m. Further, similar calculations performed for the other two fin profiles showed that the optimum fin height is around 0.025 m in all cases. This finding may be attributed to the area view factor relationship. Annular fins have an area available for conduction that increases linearly from the base to the tip. On the other hand, the surface area increases quadratically with the distance from the base. As the fin height is changed, keeping other things constant, two opposing factors come into the picture: 1) the conduction area increases linearly and tends to set up a temperature profile all along the fin; and 2) since the interaction with neighboring fins tends to oppose the radiation leaving, the temperature variation tends to decrease, which reduces the heat loss. Conduction may dominate for heights less than 2.5 cm, but the radiation interaction effect dominates beyond this point. At about 2.5 cm height, there is a balance between the two, and hence the optimum. In view of these findings, all further calculations were restricted to a fin height of 0.025 m.

Temperature profiles

Figure 7 shows the base temperature variations along the radiator for the set of parameter values shown. At each fin location, there is a large drop in temperature, indicating a comparatively large amount of heat loss from each fin as compared to the parent tube surface in between fins. This temperature drop decreases progressively as we move along the radiator, due to a decrease in the temperature along the

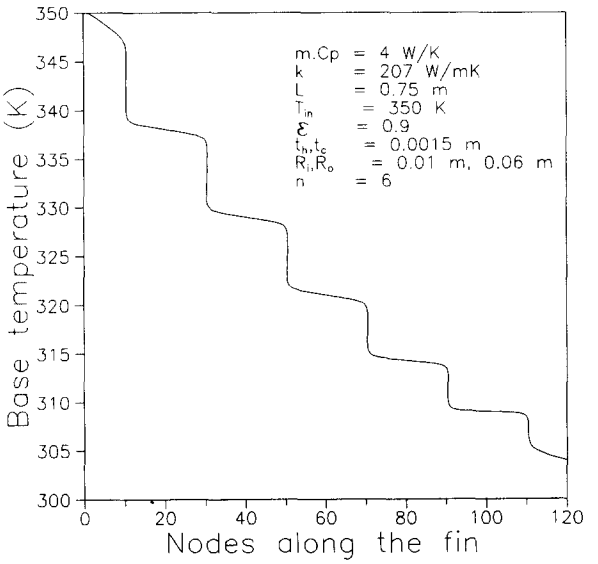

Figure 7 Temperature variation along the radiator for a typical set of parameters

radiator. In all the calculations, the base temperature of each fin is taken as the average fluid temperature based on such a temperature drop (each time taking the newly calculated higher temperature and previously calculated lower temperature and averaging them) across that particular fin. This calculation was found to produce more uniform (in a relative sense) base temperature profiles compared to those when the higher temperature alone was used for the evaluation of the fin temperature profiles, though the comparative effect of the choice of the base temperature on the total heat loss was negligible. However, in order to magnify the effects, a comparatively larger fin outer diameter along with a surface emissivity of 0.9 has been selected in Figure 7. Compared to a finned duct-type radiator considered by the authors (1992), the drops in temperature across the fins in the present case are much higher, showing thereby that annular fins are much more effective in radiating heat away. This result is primarily attributed to the area effect described by Sparrow et al. (1962). Moreover, because the fins are relatively shorter, the efficiency of the fins is high.

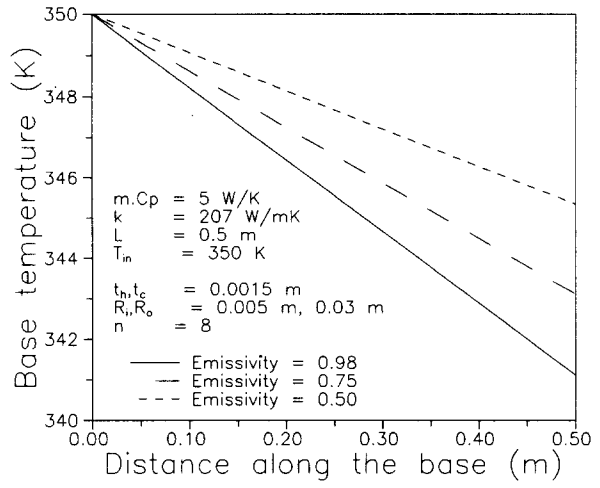

Figure 8 Effect of emissivity on the temperature variation along a tubular radiator with rectangular profile fins. R_o is chosen to have the optimum value, and the number of fins is fixed in all cases

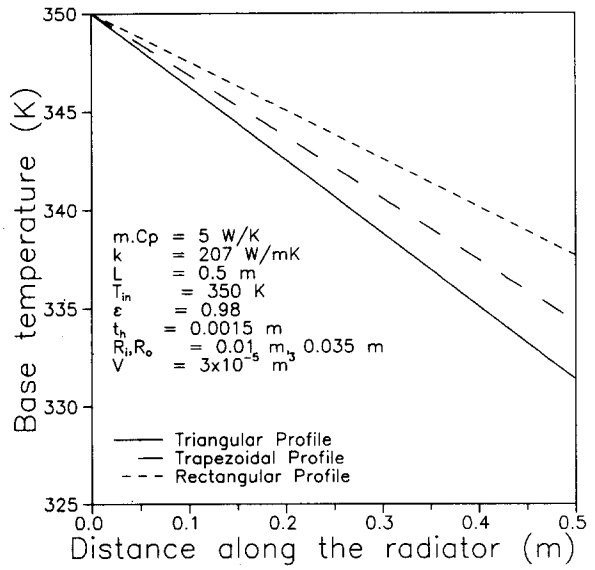

Figure 9 Temperature variation along the radiator with three different fin profiles, for a fixed fin volume in each case

The effect of emissivity on the total heat lost from the system is brought out in Figure 8. Since a higher emissivity system will lose more heat than a lower emissivity system, the outlet temperature of the former is lower than that of the latter. The three lines indicated in the figure are smoothed temperature profiles based on the actual staircase-type profile shown in the previous figure.

In Figure 9, the average base temperature variation along the radiator for three different fin profiles is given. From the figure, it can easily be concluded that the triangular-profile fin system is preferable to the other two systems because the temperature drop across it is largest for a given fin volume in the radiator. This finding can be attributed to the higher number of triangular fins that may be used in this system for a particular volume added, as well as the increase in area. This result is true in spite of the fact that the trapezoidal and rectangular profile fin cases will have more uniform fin temperature profiles. These two opposing factors (i.e., more uniform fin temperature profiles for rectangular fin geometry at the cost of a smaller number of fins for the fixed volume added), lead to the behavior shown in Figure 9.

The variation of actual temperature profile along each fin is shown in Figure 10. It can be noticed that more or less uniform distribution of temperature exists in the fins, unlike that of the flat duct-type radiator considered by the authors in their earlier work (Sunil Kumar and Venkateshan 1992). Superiority of the tubular radiator can be attributed to the higher average fin temperatures due to shorter fins. Unlike the duct-type radiator geometry, the first and the last fins in the tubular geometry do not show abnormally steeper temperature profiles. This finding also is due to relatively short fins in the system, in which the deviation of fin-tip temperatures from the base temperatures are not very significant. For taller nonoptimum fin heights, a steeper trend may be expected, as in the duct-type radiator.

The midfin temperature profiles in a tubular radiator employing three different fin geometries are shown in Figure 11. It can be noticed that, for the set of thermophysical properties shown, the base temperature for the fin is maximum

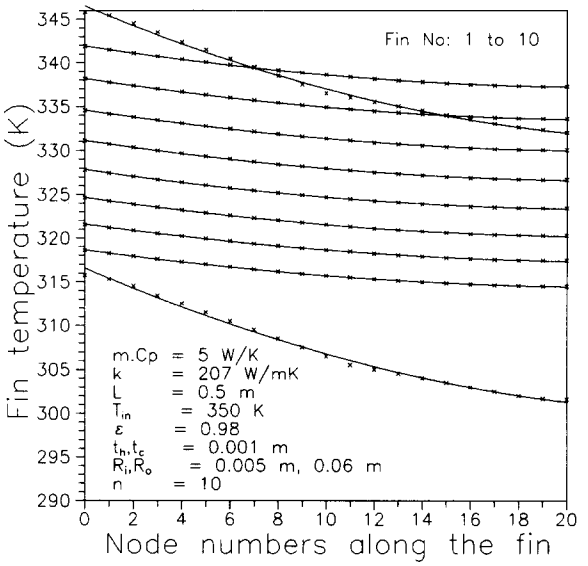

Figure 10 Temperature profiles in the fins of a radiator with 10 rectangular profiled fins

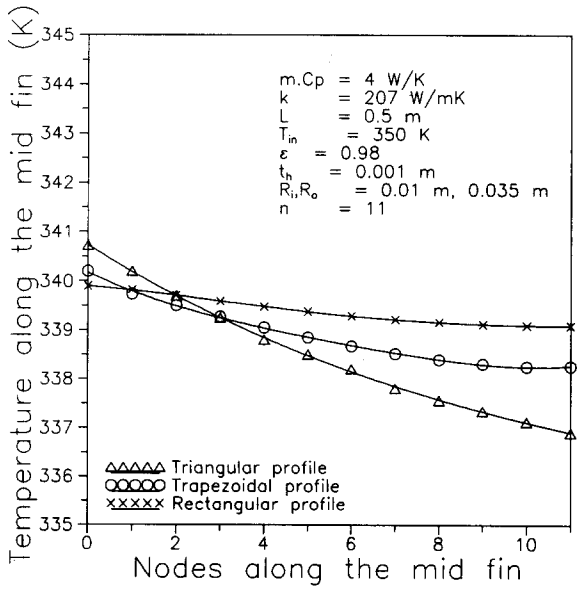

Figure 11 Midfin temperature profile for three cases of different fin profiles

for the triangular profile and minimum for the rectangular profile (the total number of fins in the three cases are held fixed at 11). This finding can be explained by looking at the fin temperature profiles. The rectangular fin has an almost uniform temperature profile compared to the other two, thus having a higher fin efficiency compared to the triangular and trapezoidal profiles. This means that more heat is lost from such a system at every fin location. Close to uniform temperature conditions prevailing in the rectangular fin may be attributed to the increased conduction area available and to multiple reflections of radiation fluxes that take place within the cavity formed by adjacent fins and the base. Therefore, at any position on the tube surface, the temperature will be lower for the system with rectangular fins as compared to the other two profiles.

Heat loss ratio and system heat loss

In Figure 12, the heat-loss ratio is plotted against the volume added, in the form of fins attached, for three different emissivities. Although a system with a higher emissivity loses more heat than a system with lower emissivity, the heat-loss ratio φ, which describes how effective the system is, decreases with increasing emissivity. This finding is attributable to the cavity effect, which varies inversely with the emissivity. In the case of a system with $\varepsilon = 0.98$, the cavity effect will not be significant, since the emissivity is already close to unity. However, when ε is small, the cavity effect is stronger and the effective emissivity is much larger than ε. Hence, the heat-loss ratio shows a relatively larger value for small emissivity values. It can be seen from the figure that the heat-loss ratio varies almost linearly with the volume of fin added.

However, it was found that heat-loss ratio tends to level off as the number of fins are increased beyond a certain number. Only a marginal increase in the effectiveness of the system takes place by the addition of fins above this number. In other words, the marginal increase in φ after this number will mean an unnecessary weight penalty and hence is not desirable from the viewpoint of design optimization. This is explained in Figure 13, where heat loss ratio is plotted against the volume of fin added. Actually, the picture will be more clear when we look at Figure 14, where the slope of the φ-vs.-volume curve is

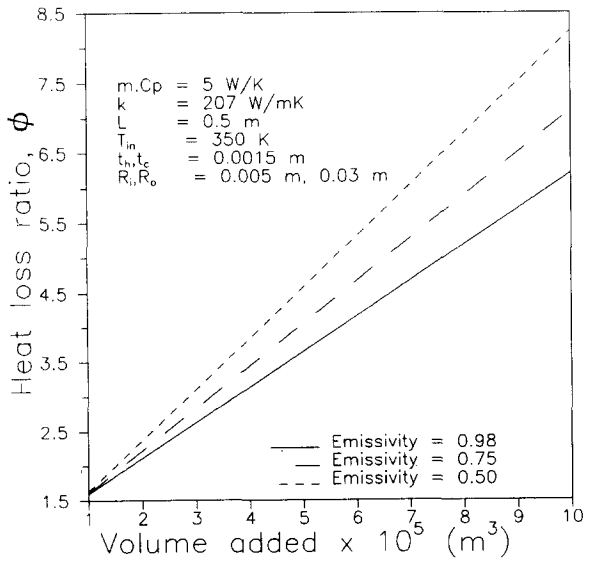

Figure 12 Dependence of heat-loss ratio on volume of fins added for various emissivities. Fins are of rectangular profile

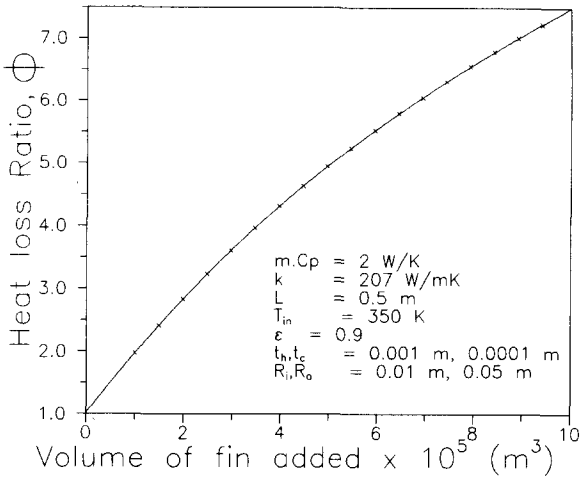

Figure 13 Relationship between heat-loss ratio and added fin volume for triangular profiled fins

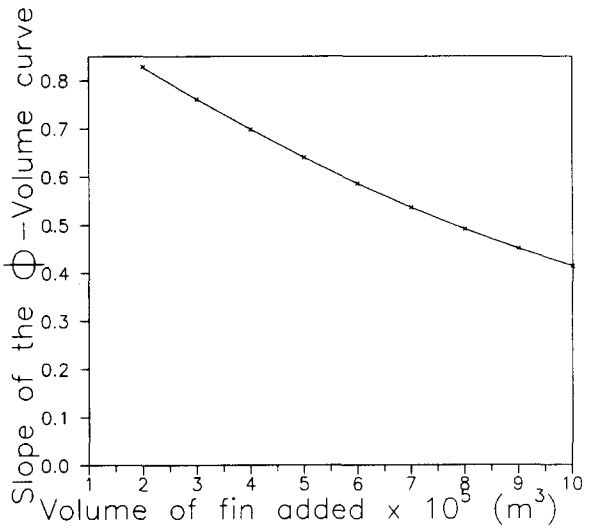

Figure 14 Slope of the curve shown in Figure 13, indicating that the heat-loss ratio saturates with increase in fin volume

plotted against the added volume itself. It is immediately apparent that as the number of fins are increased, the slope of the curve showing φ vs. number of fins decreases significantly, thus supporting the above comments. The reason that the system represented in Figure 12 does not seem to follow the above argument is because of the difference in the thermophysical parameters. Actually, this system also follows the same trend, but lies in the more linear region of the curved profile.

The effect of the variation of inlet temperature is brought out in Figure 15. Here it is seen that as the inlet temperature goes up, the effective performance value, φ, goes down. From the above two graphs, it can be concluded that the system is most efficient at a lower temperature and lower emissivities when φ is the criteria for evaluation, even though the trend of actual heat loss will actually be the opposite because at a higher temperature the system will lose more heat than at a lower temperature. The same applies to the variation with respect to emissivity. This shows that adding fins to this type of system may not be as effective at very high temperatures as at lower temperatures. This finding can be attributed to the fact that the percentage increase in the heat lost due to addition of fins

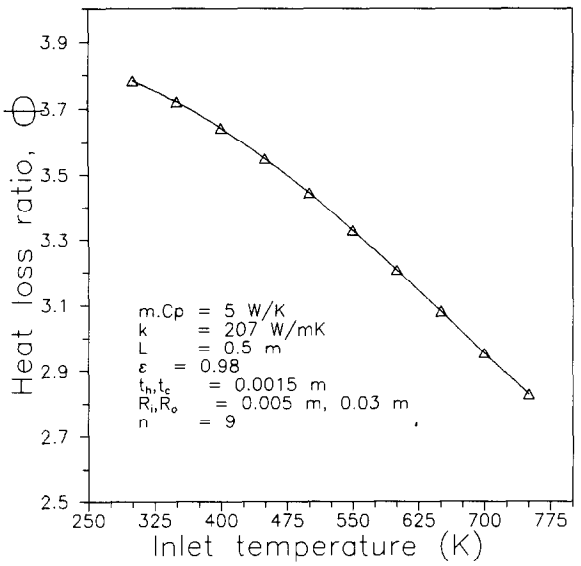

Figure 15 Variation of heat-loss ratio with inlet fluid temperature for a tubular radiator with rectangular profiled fins

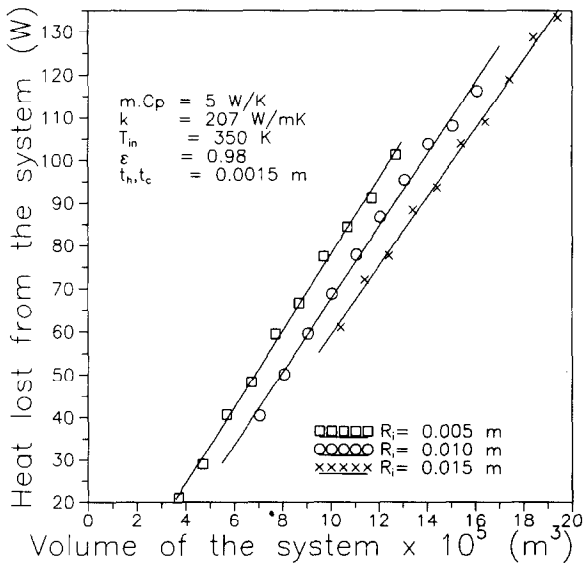

Figure 16 Performance of a radiator with rectangular profile fins with different tube diameters

is not significant compared to the total heat lost, because of the fourth power of temperature occurring in the denominator of φ.

As the tube diameter of the radiator is increased, thereby keeping the height of the fins and the volume of the system constant, the actual heat loss from the system and the heat-loss ratio decrease. The decrease in heat-loss ratio is mainly due to the tube surface-area term (which increases with diameter) in the denominator of φ. The increase in actual heat loss for the lower-diameter tube is attributed also to the increased number of fins, since the total volume of the system is fixed. In Figure 16, the actual heat lost is plotted against the volume of the system for different pipe radii. It can be seen that the heat lost from the system increases with the decrease in tube diameter, when the volume of the system (which includes both the volume of the tube and the fins attached to it) is held fixed. Figure 17 demonstrates the effect of pipe diameter on the heat-loss ratio.

It can be noticed that a system with a smaller pipe diameter should be preferred for a fixed volume of the system from the viewpoint of maximum effectiveness.

The effect of variation of mCp on the heat-loss ratio for radiators with different fin profiles is brought out in Figure 18. These calculations are all for a fixed system volume of 3×10^{-5} m^3. As expected, the triangular-profile fin system shows a definite edge over the other two systems, for the reasons explained earlier. Also, an indiscriminate increase in the mCp product will not essentially result in improving the performance coefficient of the system represented by φ. Although there is a steep increase in φ initially with an increase in mCp, after a particular point it levels off, showing that the increase of mCp after this point will not really increase the heat-loss ratio. An increase in mCp will result in the generation of a more uniform temperature profile along the base, but the initial rate of this generation cannot be sustained in later stages. This is the reason for the trends achieved in Figure 18.

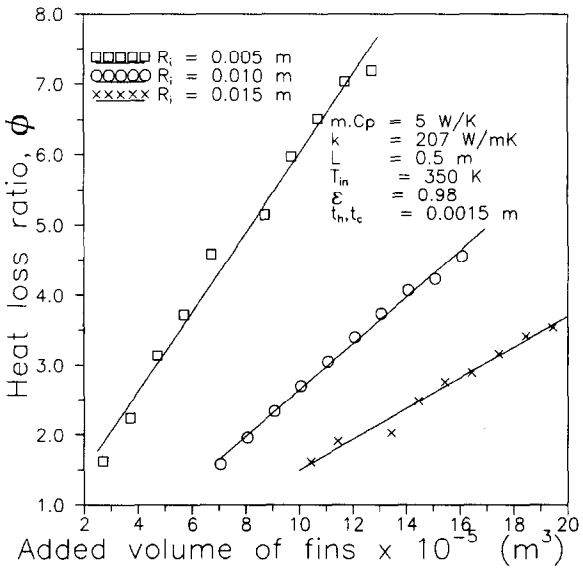

Figure 17 Performance plot shown in terms of heat-loss ratio for the cases shown in Figure 16

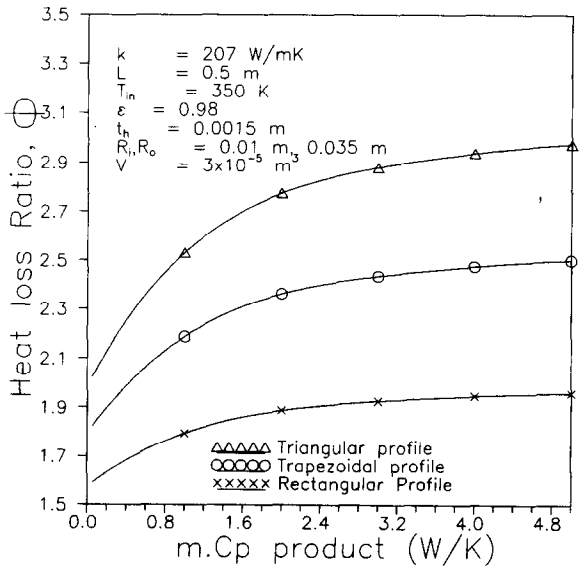

Figure 18 Variation of heat-loss ratio with mCp product for radiators with fins of three different profiles. mCp > 2 or so is not cost effective

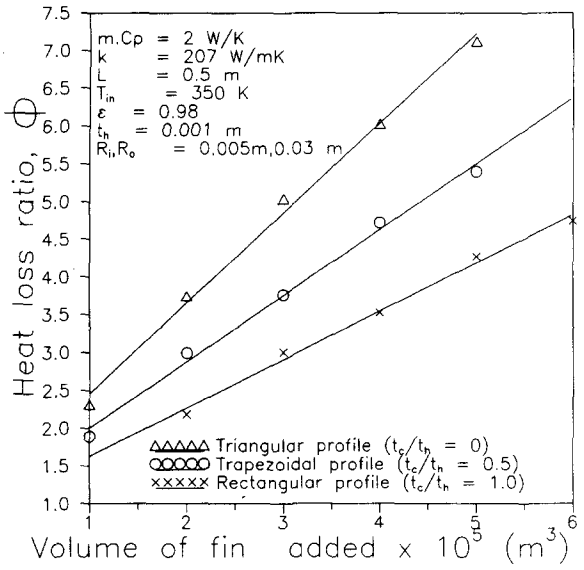

Figure 19 Variation of heat-loss ratio with volume added for the three different fin profiles

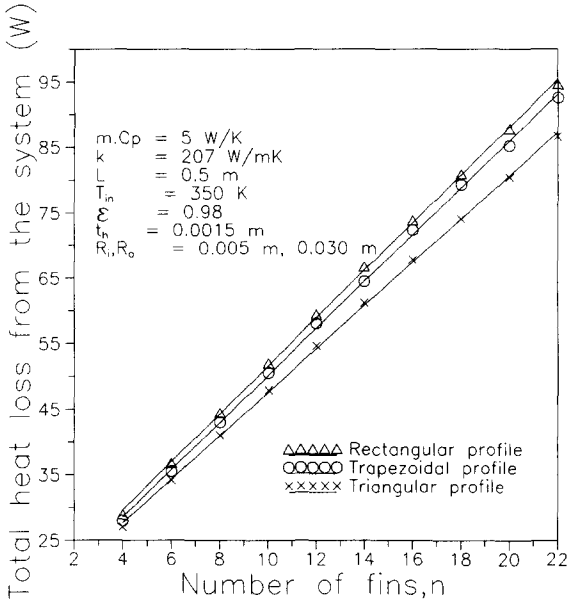

Figure 20 Performance of a system with three different fin profiles plotted against the number of fins in the system

The comparative performance of the three radiator fin geometries (triangular, trapezoidal, and rectangular) are shown in Figure 19. It can be seen that, in all the three cases as the volume added increases, there is an almost linear increase in φ. But the slopes of these lines are different, and the line with the larger slope determines which system is better. The triangular-profile fin system shows a marked improvement over the other two geometries because of the increased number of fins for a fixed volume added, and hence this system will be recommended for use from the point of view of heat transfer. The superiority of the triangular-profile fin system is achieved through a balance of the fin temperature profiles and the number of fins. This is due to the fact that the average fin temperature of the triangular-profile fin is lower than the other two, as has been illustrated earlier in Figure 11. At least for the case shown in Figure 19, it seems as though the number of fins have a more decisive role to play in the choice of fin geometry than their respective temperature profiles. Hence, the triangular fin profile is the best followed by the trapezoidal and rectangular fin profiles, in that order. The strength-criterion calculations also show that the triangular-profile fins are the best.

However, if the volume added is not a limiting factor, i.e., if the number of fins is fixed for all three cases, then the rectangular-profile fin system shows a definite superiority over the other two, viz., the trapezoidal and triangular, in that order (see Figure 20). This finding is due to the effects that have been presented and discussed earlier. Since the number of fins are held fixed, the rectangular fin profile (with a higher mean fin temperature) loses more heat than the trapezoidal and triangular fin systems.

In Figure 21, the present system is compared with a constant base temperature system (Sparrow 1962) and a conventional radiator system consisting of a tubular radiator with two longitudinal fins attached (Mackay 1963) where the total heat lost from the system is plotted against the total volume of the system. At a fixed volume, the system with constant base temperature loses more heat than a system with varying base temperature. It is evident from the figure that this difference keeps increasing with added volume. A design based on constant base temperature will then be grossly in error for the large system required to dissipate a sizable amount of heat.

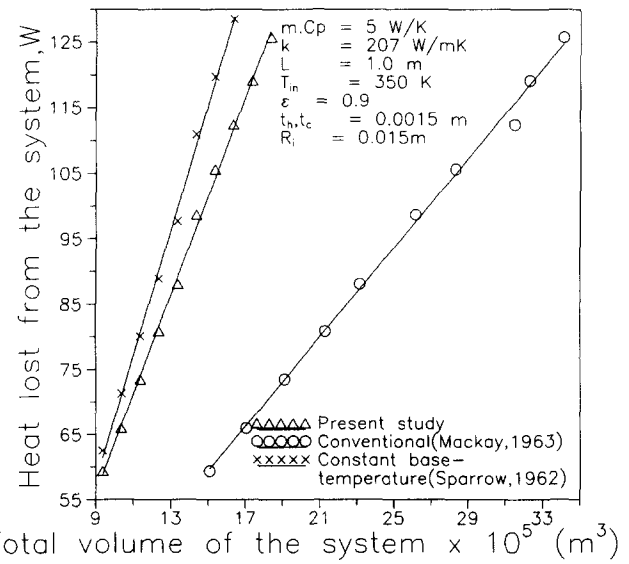

Figure 21 Comparison of performance of radiators with and without base temperature variation. Fins are of rectangular profile, and the number of fins are varied to change the system volume. Corresponding performance of a conventional radiator is also presented

From Figure 4, it is also clear that this difference or error increases with an increase in the operating temperature of the radiator, as represented by the inlet temperature of the fluid. This is due to the dependence of radiation on the fourth power of temperature, as pointed out earlier. From Figure 21, it is evident that the conventional radiator is inferior, in that much more volume is needed in the system to achieve heat loss in comparison to the other two.

Correlation

Calculations were performed for some 135 combination of parameters in each of the three different fin geometries. These

numerical results have been used to arrive at meaningful correlations that will be helpful in quick evaluation of the performance of the tubular radiator. Correlations are developed between ϕ and the other nondimensional thermophysical parameters, viz., N_{RC}, N_{CC}, geometrical parameter r_{OPT}, and the ratio of tube radius to the fin tip radius (P). The correlations are of the following general form:

$$\phi = K_1 N_{RC}^a r_{OPT}^b N_{CC}^c P^d \tag{15}$$

The constants appearing in the correlations for the three cases are given in Table 1.

The range of parameters involved in the three correlations are given in Table 2.

All the above correlations had a correlation coefficient close to 0.99, and the maximum absolute deviation was found to be less than 10 percent. The comparison of the correlated data to the numerically calculated value for the triangular geometry is shown in Figure 22 as an example.

The heat lost from the unfinned radiator is evaluated and is given in nondimensionalized form by the term β as follows:

$$\beta = \frac{1}{N_{RF}}\left[1 - \frac{1}{(1 + 3.N_{RF})^{1/3}}\right] \tag{18}$$

Design methodology

A quick design of the system may be approached in two different ways, viz., 1) based on the mass that can be added as the constraint, and 2) based on the desired heat loss as the constraint.

In the first case, one has to find out the maximum heat that can be transferred from the system for a definite mass addition, given the pipe diameter. Since volume (mass) is known, the number of fins can be found by fixing the optimum fin height at 0.025 m. Then by using the correlation, the maximum value of ϕ is evaluated. In fact, all three different geometries can be tested and the most suitable system can be chosen.

On the other hand, if one has to determine the minimum volume that is required to transfer a definite quantity of heat, one assumes the optimum fin outer diameter at the outset. The heat loss ratio, ϕ, is evaluated using Equation 18 and the known required heat loss. Since all the parameters on the right-hand side and the left-hand side of Equation 15 are known except r_{OPT}, the number of fins can be found. Once the number of fins are known, the total volume required can be evaluated. The procedure here is much easier than for the duct type radiator because in the present case the height of the fin is fixed, due to the existence of an optimum fin outer radius.

Table 1 Values for the constants in the correlations for the three cases

Profile	K_1	a	b	c	d
Triangular	0.290	−0.160	1.622	0.083	−0.316
Trapezoidal	0.391	−0.112	1.857	0.088	−0.367
Rectangular	0.510	−0.075	2.023	0.080	−0.383

Table 2 Range of parameters for the three cases

Parameter	Range
N_{RC}	$5.8 \times 10^{-5} - 6.8 \times 10^{-4}$
r_{OPT}	1.13 – 2.40
N_{CC}	$7.3 \times 10^{-3} - 3.7 \times 10^{-2}$
P	0.170 – 0.375

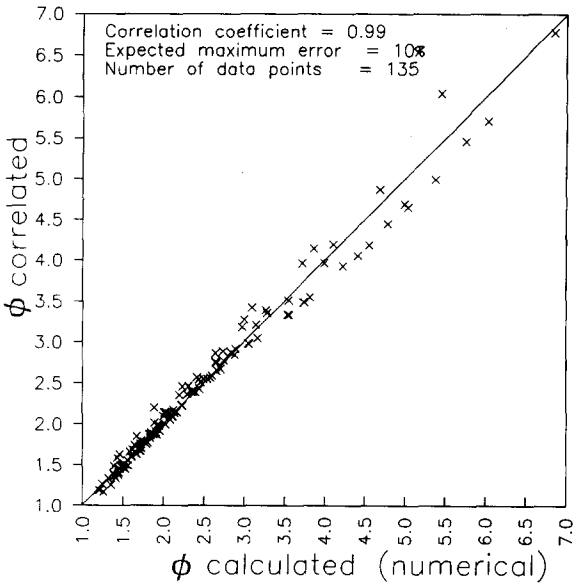

Figure 22 Parity plot showing the heat-loss ratio obtained from the correlation and the numerical data in the case of a tubular radiator with triangular profiled fins

Conclusions

A detailed analysis of an annular finned tubular radiator has been presented in this paper. An optimum fin outer diameter for a given tube diameter has been shown to exist. We have also shown that this diameter is independent of other thermophysical properties such as thermal conductivity, inlet temperature, emissivity, and the mCp product. The relative performance of the triangular-, trapezoidal-, and rectangular-profile finned radiators have been compared based on their thermal performance and the weight added. Useful correlations have been arrived at to cover a practically useful range of parameters for design as well as for evaluation of the system. A comparative study has also been performed with other available radiator models, and the superiority of the present model has been asserted. The importance of and need for the present work has also been highlighted through comparison with the earlier works. A design methodology, assuming that the local fluid bulk temperature is equal to the wall temperature, has been suggested.

Although most of the aspects of optimum design have been taken into account in this paper, it will be worthwhile to take up the following further studies with slight modifications in the program. The effect of varying fin heights from end to end in the same system (in the order of either increasing or decreasing heights), in which a better weight optimization may be possible, can be studied. An investigation can also be undertaken in which the fins are hollow and carry a boiling fluid, thereby essentially making the fin arrays isothermal and increasing the efficiency of the fins. The analysis can be extended for systems with background radiation, which can be incorporated into the program without much difficulty by specifying a nonzero background temperature.

References

Hildebrand, F. B. 1974. *Introduction to Numerical Analysis*, 2nd ed. McGraw-Hill, New York

Karlekar, B. V. and Chao, B. T. 1963. Mass minimization of radiating trapezoidal fins with negligible base cylinder interaction. *Int. J. Heat Mass Transfer*, **6**, 33–48

Keller, H. H. and Holdredge, E. S. 1970. Radiative heat transfer from annular fins of trapezoidal profile. *Trans. ASME J. Heat Transfer*, **92**, (Ser C), 113–116

Mackay, D. B. 1963. *Design of Space Power Plants*, 1st ed. Prentice-Hall, Englewood Cliffs, NJ, 221–269

Schnur, N. M. and Cothran, C. A. 1974. Radiation from an array of gray circular fins of trapezoidal profile. *AIAA J.*, **12**, 1476–1480

Schnurr, N. M., Shapiro, A. B., and Townsend, M. A. 1976. Optimization of radiating fin arrays with respect to weight. *ASME J. Heat Transfer*, **98**, 643–648

Sparrow. E. M. 1962. A new and simpler formulation for radiative angle factors. ASME paper 62-HT-17

Sparrow, E. M., Eckert, E. R. G., and Irvine, T. F. 1961. The effectiveness of radiating fins with mutual irradiation. *J. Aero Space Sci.*, **28**, 763–778

Sparrow, E. M., Miller, E. B., and Jonsson, V. K. 1962. Radiating effectiveness of annular finned space radiators. *J. Aero Space Sci.*, **29**, 1291–1299

Sunil Kumar, S. and Venkateshan, S. P. 1992. Analysis of trapezoidal finned space radiator on a non-isothermal base. Presented at ICCME '92, Nov 11–13, Singapore. *Proc. Comput. Methods Eng. Adv. Appl.*, A. A. O. Tay and K. Y. Lam (eds) (Vol. 1, 761–766), World Scientific, Singapore

Sunil Kumar, S., Venkatesh, N., and Venkateshan, S. P. 1993. Optimum finned space radiators. *Int. J. Heat Fluid Flow*, **14**, 191–200

Sunil Kumar, S. 1993. A numerical study of optimized space radiators. Ph. D. Thesis, submitted to Department of Mechanical Engineering, Indian Institute of Technology, Madras